Confinement-Induced versus

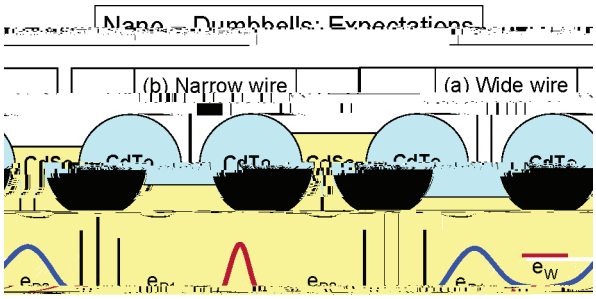

Figure 1. Schematic diagram of the energy levels and wave functions of (a) wide-wire and (b) narrow-wire nano dumbbells, where coupling between the dots and the wire is neglected. The black solid lines show the conduction-band and valence-band offsets of bulk CdTe and CdSe. The levels h_{D1} and h_{D2} are the VBM states of the two dots. The levels e_{D1}, e_{D2}, and e_W are the CBM states of the dots an the wire, respectively. In the case of a wide wire (a), the VBM wave function is localized on the dots, while the CBM wave function is localized on the wire. In the opposite case of a narrow wire (b), both the VBM and the CBM are localized on the dots.

the single-particle ground and excited states. Depending on the relative sizes R_D and R_W, the many-particle wave function (made of a coherent superposition of single-particle states) could be delocalized over the entire wire + dots system, even though the lowest-energy single-particle states are localized only on the wire or on the dots.

Although the nano dumbbell is a closed system, it is interesting to consider how it will behave electronically under transport conditions. Depending on the kinetics of carrier injection, the system can contain either one or several electrons.[15] The spatial localization of the electrons is controlled by quantum confinement and correlation effects. For example, if the nano dumbbell contains two electrons, then for a narrow wire the natural propensity will be for each dot to contain one electron, whereas for a wide wire both electrons will be in the wire. External bias, under transport conditions, will have to overcome such energetic preferences that are induced by many-particle effects. Yet, the spatial distribution of carriers is often described theoretically via one-particle effects alone. What we propose here is a general approach that describes quantitatively the balance between one-electron and many-electron effects and can accurately predict the degree of carrier localization and wave function entanglement in complex nanostructures. The only input to the calculation is the composition, shape, and size of the nanostructures. Thus, if those are determined experimentally for a series of nanostructures, then we can identify which will be dominated by single-particle effects and which will be dominated by correlation effects.

Several methodologies are available in the literature for combining a single-particle description with a many-body treatment. "First-generation" approaches are based on continuum effective-mass single-particle theories, such as the one-band particle-in-a-box effective-mass approximation (see, e.g., ref 16) or the few-band **k.p** approximation (e.g., ref 17). These continuum-like effective-mass approaches have been combined with many-body treatments such as quantum Monte Carlo[18] or configuration interaction (either for **k.p**[19] or for the single-band effective mass[20]), enabling calculations of large (up to 10^7 atoms) systems. These single-particle approaches model quantum confinement but either neglect[16] or oversimplify[17] the effects of interband coupling (i.e., the coupling between various bands at a given point of the Brillouin zone), intervalley coupling (e.g., the coupling between the ¡, X, and L valleys), and strain. These approximations lead to quantitative[21]—and often even qualitative[22]—errors in the single-particle energies and wave functions. For example, simple effective-mass models do not include heavy hole/light hole mixing, which is primarily responsible for the bonding−antibonding splitting of the hole states in dot molecules.[23] "Second generation" approaches are based on atomistic single-particle theories (such as tight-binding[24] or empirical pseudopotentials[25]), which include a broad range of single-particle effects (e.g., interband and intervalley coupling, strain, compositional inhomogeneity), albeit via empirical parametrization of the bulk Hamiltonian. These approaches have also been combined with many-body approaches, such as configuration interaction (either in the context of tight-binding[26] or pseudopotentials[27]), enabling calculations on 10^3-10^6 atom systems. What we are aiming at is a "third-generation" approach, based on first-principles atomistic single-particle theories, such as density-functional theory in the local-density approximation (LDA), combined with a sophisticated many-body approach. To date, such combinations of methodologies are limited to tiny nanostructures,[28,29] because both the single-particle LDA method and the many-body approaches are enormously demanding from a computational point of view. Here we combine an atomistic, LDA-quality single-particle "charge-patching" approach[30] with a configuration-interaction many-particle method[27] to calculate quantum confinement and electron localization in semiconductor nano dumbbells containing up to 6000 atoms.

We consider semiconductor nano dumbbells consisting of two nearly spherical CdTe dots of radius $R_D = 25$ Å, connected by a 30-Å-long CdSe wire of variable radius R_W. CdTe quantum dots are usually grown in the zinc blende lattice structure. Here we assume that the CdSe wire is grown pseudomorphically along the (100) crystallographic orientation and that it inherits the zinc blende lattice structure of the CdTe dots. Surface atoms are passivated using a ligandlike potential,[31] which acts to remove surface states from the band gap. Figure 2 shows the atomistic structure of one of the nano dumbbells used in the calculations ($R_W = 10$ Å). This system consists of 2268 Cd atoms, 2100 Te atoms, 169 Se atoms, and 1436 passivants, for a total of 5973 atoms. The atomic positions are relaxed using an atomistic valence force field model. The parameters of this model are fitted to the bulk elastic constants of the constituents. The

total valence charge density of the relaxed system is then constructed using the charge-patching method.[30] In this method, small prototype systems with similar local atomic structures as the dumbbell are calculated self-consistently using LDA. The total charge density of these prototype systems is decomposed into charge-density motifs belonging to different atoms. These charge motifs are then assembled to generate the total charge density of the dumbbell. The typical density error generated this way is less than 1% compared to direct LDA calculations.[30] After the charge density is obtained, the LDA is used to generate the total electronic potential. The ensuing single-particle Schroedinger equation is then solved using the folded spectrum method[25]

3), which depend on the spatial variable r and the spin variable σ, and $\ldots_{jl}(r$

singlet state slightly lower in energy than the triplet state), as a result of electron−electron repulsion. The next two states correspond to the two electrons being localized on the same dot. The localization of the electrons on opposite dots is driven by correlation effects, as demonstrated by the correlation function plot shown at the bottom of Figure 6. When one electron is located at the center of the left-hand side dot (blue circle), then the second electron (yellow cloud) is delocalized on both dots in the uncorrelated case, but only on the right-hand side dot in the correlated case.

Finally, we consider the case of intermediate wire thickness (Figure 7). In this case there are several two-electron configurations in a narrow (<100 meV) energy window (Figure 7a). Direct Coulomb interactions change the order of the configuration energies (Figure 7b). In particular, the configuration $|\psi_1\psi_2\rangle$ is pushed lower in energy than $|\psi_1\psi_1\rangle$, as a result of reduced Coulomb repulsion (83 vs 150 meV). Configurations that are 4-fold degenerate (due to spin degeneracy) at the single-particle level (Figures 7a and 7b) split into a singlet and a triplet in the single-configuration approximation (Figure 7c). The ground state is the triplet state originating from the configuration $|\psi_1\psi_2\rangle$. The next two excited states are also triplet states, originating from the configurations $|\psi_1\psi_3\rangle$ and $|\psi_2\psi_3\rangle$, respectively. Configuration interaction mixes states of the same spin multiplicity, leading to a ground state that has contributions from several configurations ($|\psi_1\psi_1\rangle$, $|\psi_1\psi_3\rangle$, and $|\psi_2\psi_2\rangle$), as shown in Figure 7d. Strong correlation effects alter the distribution of the two electrons. A plot of the correlation function (bottom of Figure 7) shows that while the two electrons are mainly localized on the wire in the uncorrelated case they are located on the dots when configuration interaction is taken into account. The degree of entanglement in this case has an intermediate value of 61%, showing a certain mixing of configurations that does not lead, however, to a purely symmetric or antisymmetric state with maximum entanglement. The next excited state originates from the $|\psi_1\psi_2\rangle$ triplet states with some admixture of $|\psi_2\psi_3\rangle$ character (Figure 7d). These 3-fold degenerate states have a degree of entanglement between 80% and 97%.

The localization of the single-particle wave functions has direct consequences on the optical properties of the nano dumbbells. As the wire becomes narrower, the CBM wave function migrates from the CdSe wire to the CdTe dots, while the VBM wave function remains localized on the CdTe dots, as shown in Figure 3. Thus, the band alignment of the

CdTe dots, resulting in a relatively large electron−hole binding energy ($E_b = 115$ meV). As the CdSe wire becomes wider, the exciton binding energy decreases to 86 meV for $R_W = 10$ Å and 59 meV for $R_W = 15$ Å.

In conclusion, we have shown that the localization of the single-particle wave functions in CdSe/CdTe nano dumbbells can be controlled by changing the radius of the CdSe wire. As the wire becomes narrower, the wire electron states are pushed higher in energy compared to the dot electron states, so the lowest electron state changes its localization from the wire to the dots. We have also demonstrated that, when the radius of the CdSe wire is small ($R_W \leq 10$ Å), strong correlation effects determine the spatial localization and the degree of entanglement of the two-electron wave functions. As previously shown,[36] carrier localization and wave function entanglement are not “frozen in” for a given nanostructure composition, shape, and size but can be deliberately tuned by applying an external electric field. Our methodology provides an accurate way to characterize the most important features that are currently not accessible experimentally, i.e., the degree of carrier localization and wave function entanglement. Our results illustrate how complex semiconductor nanostructures such as nano dumbbells can serve as a platform to simultaneously manipulate quantum confinement, electron−electron correlation, and wave function entanglement and can provide the basic architectural elements of nanodevices.

Acknowledgment. This work was supported by the DOE-SC-BES initiative LAB03-17, under NREL Contract No. DE-AC36-99GO10337.

References

(1) Collins, P. G.; Avouris, P. *Sci. Am.* **2000**, *283*, 62.
(2) Huang, Y.; Duan, X.; Cui, Y.; Lauhon, L. J.; Kim, K. H.; Lieber, C. M. *Science* **2001**, *294*, 1313.
(3) Klein, D. L.; Roth, R.; Lim, A. K. L.; Alivisatos, A. P.; McEuen, P. L. *Nature* **1997**, *389*, 699.
(4) (a) Tarucha, S.; Austing, D. G.; Honda, T.; van der Hage, R. J.; Kouwenhoven, L. P. *Phys. Rev. Lett.* **1996**, *77*, 3613. (b) Kouwenhoven, L. P.; Oosterkamp, T. H.; Danoesastro, M. W. S.; Eto, M.; Austing, D. G.; Honda, T.; Tarucha, S. *Science* **1997**, *278*, 1788.
(5) Warburton, R. J.; C Schaflein, Haft, D.; Bickel, F.; Lorke, A.; Karrai, K.; Garcia, J. M.; Schoenfeld, W.; Patroff, P. M. *Nature* **2000**, *405*, 926.
(6) Reuter, D.; Kailuweit, P.; Wieck, A. D.; Zeitler, U.; Wibbelhoff, O.; Meier, C.; Lorke, A.; Maan, J. C. *Phys. Rev. Lett.* **2005**, *94*, 026808.
(7) *International Technology Road Map for Semiconductors*. http://public.itrs.net.
(8) Loss, D.; DiVincenzo, D. P. *Phys. Rev. A* **1998**, *57*, 120.
(9) Bimberg, D.; Ledentsov, N. N.; Grundmann, M. *Quantum Dot Heterostructures*; Wiley: New York, 1999.
(10) Lieber, C. M. *MRS Bull.* **2003**, *28*, 486.
(11) Bastard, G. *Wave Mechanics Applied to Semiconductor Heterostructures*; Les Editions de Physique: Les Ulis, France, 1988.
(12) (a) Yannouleas, C.; Landman, U. *Phys. Rev. Lett.* **1999**, *82*, 5325. (b) Troiani, F.; Hohenester, H.; Molinari, E. *Phys. Rev. B* **2002**, *65*, 161301. (c)